

University of Dundee

## Field investigation of deformation characteristics and stress mobilisation of a soil slope

Leung, Anthony Kwan; Ng, Charles Wang Wai

*Published in:*  
Landslides

*DOI:*  
[10.1007/s10346-015-0561-x](https://doi.org/10.1007/s10346-015-0561-x)

*Publication date:*  
2015

*Document Version*  
Peer reviewed version

[Link to publication in Discovery Research Portal](#)

### *Citation for published version (APA):*

Leung, A. K., & Ng, C. W. W. (2015). Field investigation of deformation characteristics and stress mobilisation of a soil slope. *Landslides*. <https://doi.org/10.1007/s10346-015-0561-x>

### **General rights**

Copyright and moral rights for the publications made accessible in Discovery Research Portal are retained by the authors and/or other copyright owners and it is a condition of accessing publications that users recognise and abide by the legal requirements associated with these rights.

- Users may download and print one copy of any publication from Discovery Research Portal for the purpose of private study or research.
- You may not further distribute the material or use it for any profit-making activity or commercial gain.
- You may freely distribute the URL identifying the publication in the public portal.

### **Take down policy**

If you believe that this document breaches copyright please contact us providing details, and we will remove access to the work immediately and investigate your claim.

1        **The final publication is available at Springer via <http://dx.doi.org/10.1007/s10346-015-0561-x>**

2

1                   **Field investigation of deformation characteristics and stress mobilisation of a soil slope**

2                   Anthony, Kwan Leung\* and Charles, Wang Wai Ng

3  
4   **Name:** Dr Anthony Kwan, LEUNG\* (Corresponding author)

5   **Affiliation:** Lecturer, Division of Civil Engineering, University of Dundee

6   **Address:** Fulton Building, Division of Civil Engineering, University of Dundee, Nethergate, UK, DD1 4HN

7   **E-mail:** [a.leung@dundee.ac.uk](mailto:a.leung@dundee.ac.uk), **Telephone:** +44(0)1382 384390, **Fax:** +44(0)1382 384389

8  
9   **Name:** Dr Charles Wang Wai, NG

10   **Affiliation:** Chair Professor of Civil and Environmental Engineering, Department of Civil and Environmental  
11   Engineering, Hong Kong University of Science and Technology

12   **Address:** Department of Civil and Environmental Engineering, Hong Kong University of Science and  
13   Technology

---

14  
15   **Abstract**

16   Stress mobilisation and deformation of a slope are important for engineers to carry out reliable design of  
17   retaining systems. However, most case histories reported mainly on the response of pore-water pressure (PWP),  
18   whereas knowledge about the stress-deformation characteristics of slope is limited. In this study, a saprolitic soil  
19   slope was instrumented to monitor not only the responses of PWP but also horizontal stress and horizontal  
20   displacement. To assist in the interpretation of field data, a series of laboratory tests was conducted to  
21   characterise the volume change behaviour of soil taken from the site, under the effects of both net stress and  
22   suction. During a rainstorm event when positive PWP built up, a remarkably large displacement of 20 mm was  
23   recorded between 5.5 and 6 m depths, and the top 5 m of the slope exhibited translational down-slope movement.  
24   This caused an increase in effective horizontal stress by 350%, which reached a peak value close to 40% of an  
25   effective passive stress. During the subsequent dry season when suction was recovered, an up-slope rebound of  
26   10 mm was recorded. Comparison of field and laboratory data reveals that the rebound was attributed to  
27   suction-induced soil shrinkage. This rebound led to a decrease in the effective horizontal stress previously built  
28   up during the storm event.

29  
30   **KEYWORDS:** Deformation, Slope ratcheting, Stress mobilisation, Suction, Saprolitic soil, Field monitoring

---

## 1 Introduction

2 Rain-induced slope failure is increasingly reported in the past 20 years, especially in tropical regions like  
3 Singapore and Malaysia, and sub-tropical regions like Hong Kong and Brazil. This natural hazard has caused  
4 huge socio-economic losses (Sassa and Canuti 2008). It has been predicted that over the next 50 years, rainfall  
5 will be more intense (IPCC 2007), imposing an increased threat to slope stability. Because of the global climate  
6 change, improving the understanding of seasonal slope behaviour is necessary because seasonal fluctuation of  
7 pore-water pressure (PWP) directly affects soil shear strength mobilised for resisting rain-induced slope failure.  
8 Centrifuge tests conducted by Take and Bolton (2011) have revealed that seasonal drying-wetting events could  
9 promote progressive failure of a soil slope due to the repeated mobilisation of dilatancy in successive wet  
10 seasons. However, comprehensive field studies that cover the monitoring of slope responses during both dry and  
11 wet seasons are scarce, especially those related to the stress-deformation characteristics of the slopes.

12 In the literature, most of the case histories focused on the monitoring of hydrologic responses, including  
13 PWP, soil water content and groundwater level during wet seasons in slopes comprising of residual soils (Lim et  
14 al. 1996), decomposed soils (Kim and Lee 2010; Leung et al. 2011), non-expansive clay (Smethurst et al. 2006)  
15 and expansive clay (Ng et al. 2003). On the contrary, field studies of the mechanical slope behaviour (i.e.,  
16 stress-deformation characteristics) are rare. A field study conducted by Ng et al. (2003) is one of the few case  
17 histories measuring the mobilisation of soil stress during rainfall. It is revealed that there was a significant  
18 increase in total horizontal stress ( $>$  three times higher than the total vertical stress) when a clayey slope was  
19 subjected to a rainfall event with average daily amount of 62 mm for seven days. The mobilised stress ratio was  
20 close to an effective passive stress ratio, indicating the possibility of passive failures of the clay. It is thus crucial  
21 to quantify the amount of a stress mobilised in slope during rainfall for engineers to carry out reliable design for  
22 their slope retaining systems.

23 Recently, a slowly-moving landslide body was identified in a saprolitic soil slope situated at Tung Chung,  
24 Lantau Island in Hong Kong (Fig. 1). Slope failure from the site is categorised to impose “high” risk and losses  
25 to the society because the failure mass could block the North Lantau Highway, which is the critical transport  
26 corridor to the Hong Kong International Airport. On 7 June 2008, an extreme storm event (maximum one-hour  
27 rainfall of 133 – 140.5 mm with corresponding return period exceeding 240 years) resulted in a total of 38  
28 landslides occurring on the hillside above the Highway (AECOM 2012). Four of them developed into  
29 channelized debris flows, which transported about 540 m<sup>3</sup> of sediment downstream. Although no casualties  
30 were reported, the debris hit the Highway closing it for about 16 hours. Through detailed monitoring of the

---

landslide body, Leung et al. (2011) and Leung and Ng (2013a) interpreted the responses of PWP and soil water content to deduce some groundwater flow mechanisms during a storm event. These mechanisms were later confirmed by detailed two- and three-dimensional anisotropy seepage analyses conducted by Leung and Ng (2013b).

This study focuses on and explores the seasonal effects on deformation characteristics and the associated stress mobilization of the research slope based on the existing frameworks of saturated and unsaturated soil mechanics. Stress mobilised during an alternative dry/wet season is interpreted in relation to the responses of PWP and slope displacement. The characteristics of slope deformation are studied by comparing field monitoring data with laboratory measured volumetric behaviour of soil taken from the landslide body. In this study, the following effective stress principle in Eq. 1 is adopted to interpret the slope behaviour.

$$\sigma' = (\sigma - u_a) + \chi(u_a - u_w) \quad (1)$$

$$\text{where } \chi = \begin{cases} 1, & \text{when } S_r = 100\% \\ \left(\frac{s_e}{s}\right)^\gamma, & \text{when } S_r < 100\% \end{cases}$$

where  $u_a$  is pore-air pressure;  $u_w$  is PWP;  $\sigma$  is total stress;  $(\sigma - u_a)$  is net stress;  $(u_a - u_w)$  is matric suction,  $s$ ;  $\chi$  is Bishop's parameter;  $s_e$  is air-entry value;  $S_r$  is degree of saturation; and  $\gamma$  is 0.55 (Khalili and Khabbaz 1998), which is a coefficient that has been calibrated against the shear strength of a broad range of soil types. Note that the use of Eq. 1 aims to interpret the field dataset by linking PWP (positive or negative) with stress mobilised in the slope qualitatively. It is, however, not the scope of this study to use a sophisticated soil model to carry out detailed hydro-mechanical analysis for the slope quantitatively.

## Site description and ground profile

The overview of the study area is shown in Fig. 1. The slope is located at Tung Chung, Lantau Island in Hong Kong and faces the Tung Chung Eastern Interchange. The slope forms a blunt ridgeline located between a stream channel to the north-east and a shallow topographic valley to the south-west. The average slope gradient is 30°. The slope is moderately to densely vegetated and it is a typical short shrubland, predominantly covered by fern and woody species (Leung and Ng 2013b). At the mid-portion of the study area, a 45 m wide, 50 m long landslide body was identified (see the inset). A series of sub-parallel tension cracks contouring the hillside of approximately 45m wide were found at elevations between +84 to +86 mPD (mPD stands for metres above Principle Datum and it refers to an elevation 1.23m above mean sea level; SMO 1995). Some lateral tension cracks were present along both the eastern and western flanks of the landslide body. At +64 mPD, some thrust

features were identified.

A ground profile across section A-A is depicted in Fig. 2. In the top 2 to 3 m of the slope, colluvial deposit, which consists of silty clay mixed with some cobbles of decomposed tuff, were encountered. Below the colluvium stratum, a thick stratum of saprolites, namely completely decomposed tuff (CDT), was found to overly a 3 – 4 m thick stratum of highly decomposed tuff (HDT). At distance of 20 m, there is a substantial drop of the profile of the underlying moderately to slightly decomposed tuff (MDT/SDT), which is classified as rock. Through trial trench exploration, rupture surfaces were identified near the colluvium-CDT interface at 2 – 4 m depths. The inferred landslide body and some of its features are shown in Fig. 2. Initial monitoring of the groundwater level (GWL) before the start of the monitoring showed that it was at about 11 m depth and nearly followed the rock head profile of MDT/SDT.

### Soil properties

Block samples at 0.5, 1, and 2 m depths were collected at the research slope for measuring index properties, effective strength parameters and volumetric behaviour of colluvium and CDT in the laboratory. It is found that the in-situ water content (by mass) of colluvium was about 20% (slightly higher than the plastic limit of 17%), while that of CDT varied from 17% to 22% (the average of which is close to the plastic limit of 20%). On the other hand, the in-situ dry density of colluvium ( $1.5 \text{ g/m}^3$ ) and CDT ( $1.6 \text{ g/m}^3$ ) was about 95% and 90% of their maximum value obtained from Standard Proctor Tests, respectively. Figure 3 shows the particle-size distributions (PSDs) of colluvium and CDT. The average gravel, sand, silt, and clay contents of colluvium are 18%, 25.5%, 39.5% and 17%, respectively. On the contrary, the PSD of CDT appears to be consistent among the block samples, having the gravel, sand, silt, and clay contents of 2.5%, 35%, 42.5%, and 20%, respectively. According to the Unified Soil Classification System, both colluvium and CDT are classified as CL. Shear strength parameters of saturated colluvium and CDT were determined through consolidated undrained (CU) triaxial tests. Figure 4 shows the Mohr-Coulomb envelopes of both materials. The test results show that the effective cohesion,  $c'$ , and the effective friction angle,  $\phi'$ , of colluvium are 0.3 kPa and  $35.2^\circ$ , respectively, while those of CDT are 7.4 kPa and  $33^\circ$ , respectively. Table 1 summarises the index properties of colluvium and CDT.

A series of laboratory tests were conducted to measure the soil water retention curve (SWRC) and to characterise volumetric behaviour of colluvium and CDT. SWRC is an unsaturated hydraulic property that reflects the water retention ability of an unsaturated soil for any given suction and net stress. A pressure-plate device (Ng and Pang 2000) adopts axis-translation technique (Hilf 1956) to independently control net stress ( $\sigma$ –

$u_a$ ) and suction ( $u_a - u_w$ ), which are generally recognised to be the two stress-state variables that govern the behaviour of an unsaturated soil (Coleman 1962). Each sample was trimmed into an oedometer ring and was saturated before testing. Each CDT sample was consolidated at a vertical net stress under  $K_0$  condition at 40 or 80 kPa, which represents the approximate in-situ overburden pressure at 2 and 4 m depths, respectively. In contrast, no vertical net stress was applied to the colluvium specimen as it existed in shallow depths of the slope. Any effects of overburden pressure on SWRC and volumetric behaviour of colluvium may be negligible. After consolidation, step increases in suction from 0 to 400 kPa were applied to each sample to undergo a drying path, while any vertical net stress applied was maintained throughout the test. At each equilibrium suction step, water content and vertical displacement of each sample were recorded. When suction of 400 kPa was reached, similar test procedures were adopted for a wetting path. In this case, suction was controlled to reduce suction from 400 to 0 kPa in steps. More details of test procedures were reported by Ng and Pang (2000).

Figure 5(a) shows the SWRCs of both colluvium and CDT. Each SWRC was fitted with the equation proposed by van Genuchten (1980), and all the associated parameters are listed in Table 2. It can be seen that the air-entry value of colluvium and CDT is  $\sim 1$  and 2 kPa. For a given increase in suction, the desorption rate of CDT is less than that of colluvium, most likely because the fine content in CDT is higher. Hydraulic hysteresis is observed in both materials, but the difference of  $S_r$  along the drying and wetting SWRC is less than 20%. Figure 5(b) shows the variations of void ratio of each sample with suction. The observed different initial void ratio (at zero suction) was attributed to the different net stresses applied to each sample. The higher the applied stress, the lower the void ratio should be. At zero net stress, the void ratio of colluvium reduced by 7.2% when the applied suction increased from 3 to 400 kPa. By defining the gradient of the log-linear portion of the curve as soil shrinkability,  $\lambda_s$ , the  $\lambda_s$  for this case is  $0.0406 (\log \text{ kPa})^{-1}$ . For CDT loaded at higher net stresses of 40 and 80 kPa, similar variations of void ratio are observed. However, the  $\lambda_s$  was lower as CDT loaded to a higher stress level has higher stiffness to resist soil volume change due to suction increase (Ng and Yung 2008). At 80 kPa of net stress, the reduction of void ratio (3.5%) of CDT was only half of that of colluvium for the same increase in suction. Along the wetting path, only a slight increase in void ratio (i.e., swelling) is observed for all specimens during the initial wetting, but when suction was less than 10 kPa, no swelling is observed.

## Arrangement of instruments

As shown in Fig. 2, three jet-fill tensiometers (JFTs) were installed at the central portion of the landslide body to measure negative PWP in colluvium at 0.5 and 1.5 m depths and CDT at 2.5 m depth. Due to the possibility of

cavitation of water, the minimum PWP that can be recorded by each JFT is not less than -90 kPa. The accuracy and resolution of each JFT are both  $\pm 1$  kPa. During the monitoring period, any accumulated air bubbles due to cavitation and air diffusion in each JFT were removed by pressing the jet-fill button. Three time domain reflectometers (TDRs) were installed 0.5 m away from the three JFTs to measure volumetric water content (VWC) at 0.5, 1.5 and 2.5 m depths. Each TDR was calibrated in laboratory and the accuracy of each TDR is within 2% for VWCs ranging from 10% to 40%.

In order to monitor changes of GWL, six piezometers (CPs) and a standpipe (SP) were installed. Each piezometer consists of a vibrating-wire type pressure transducer to record positive PWP. Any increase in positive PWP is equivalent to an increase in GWL with reference to the installation depth of each piezometer. Two piezometers, namely S-CP<sub>ce</sub> and S-CP<sub>th</sub>, were installed at shallower depth at 4 m near the colluvium-CDT interface, while the other four, namely CP<sub>cr</sub>, CP<sub>ce</sub>, CP<sub>th</sub> and CP<sub>toe</sub>, and the SP were installed in deeper depths (8 to 11 m depths) to monitor the responses of the GWL at various locations along the slope.

A pair of earth pressure cells (EPCs) was installed at a 2 m depth in the central portion of the landslide body to monitor the responses of total horizontal stress. The two EPCs were installed perpendicular to each other so that one of them measured total horizontal stress in the down-slope direction ( $\sigma_D$ ), while the other one measured in the cross-slope direction ( $\sigma_C$ ). At the installation location, a 1 m x 1 m (in plan) trial pit was excavated to a depth of 2.5 m, which is within the maximum depth of 4.5 m recommended by Eurocode 7 BS EN1997-1 (BSI 2004). At 2 m depth, a slot with a size similar to the width of each EPC was cut and the EPC was inserted into the slot. Inevitably, these procedures caused stress release around the slot and hence, the initial total horizontal stress recorded by each EPC was reduced to zero. Thus, subsequent reading represents change of horizontal stress with reference to the initial zero total stress. To provide better contact between each EPC and the surrounding soil, the gap between them was filled with cement bentonite grout. This allowed tensile stresses to be transmitted between each cell and the surrounding soil (Brackley and Sanders 1992; Ng et al. 2003).

To monitor the total horizontal displacement of the slope, two in-place inclinometers (IPI) were installed at the central portion (IPI<sub>ce</sub>) and near the thrust features (IPI<sub>th</sub>) of the landslide body. Four tilt accelerometers were mounted near the ground surface, at 1, 3 and 5 m depths along each IPI casing. As slope displaces, each tilt accelerometer would record tilt angle with respect to the vertical axis of the casing. For the given spacing of accelerators and measured tilt angles, horizontal displacements (accuracy of  $\pm 0.01$  mm) at the depth of each accelerator installed can be determined. The only difference of the working principle of an IPI from a manual one is that measurements made by the former are automatic, whereas the latter requires manual surveying. Note



that the horizontal displacement measurements made before the storm event in June 2008 were referenced to 7 m depth, where zero displacement was assumed for both IPIs. After the storm event, the IPI<sub>ce</sub> recorded large slope displacements in the top 5 m (as discussed later), and therefore two extra tilt accelerometers were installed at 7 and 10 m depths on January 2009. Zero displacement was assumed at a 13 m depth thereafter.

## **Interpretation of slope behaviour during wet period**

### *Observed slope responses during the wet season*

Figures 6(a) and (b) show the variations of PWP and VWC with rainfall, respectively. During the wet period from May to July 2008, consistent responses between PWP and VWC are observed at all three depths (0.5, 1.5 and 2.5 m). When rainfall happened, PWP increased simultaneously with an increase in VWC. It can be seen in Fig. 6(a) that PWP at 1.5 and 2.5 m depths respectively reached peak positive value of 12 and 20 kPa, when subjected to the storm with rainfall intensity of 133.5 mm/hr (equivalent to return period of 245 years) on 7 June. This corresponds to almost the same peak VWC of 36% (Fig. 6(b)). The observed maximum VWC in the field is found to be close to the saturated VWC obtained in the laboratory (Ng et al. 2011). This suggests that the soil at these two depths should have been saturated when positive PWP was recorded. Seepage analyses conducted by Leung and Ng (2013b) have shown that the amount of rainfall was sufficient to develop a perched water table at the colluvium-CDT interface, which caused the significant increase in PWP at a depth of 2.5 m. However, since the measurements of PWP and VWC were recorded at 0.5, 1.5 and 2.5 m depths, they may reflect the saturation condition in the top 2.5 m of the soil only.

Figure 6(c) shows the seasonal horizontal displacement at various depths (i.e., ground surface, 1, 3 and 5m) observed at the central portion (IPI<sub>ce</sub>) and near the thrust features (IPI<sub>th</sub>) of the landslide body. An increase in displacement means that the soil displaces towards the down-slope direction. When the extreme storm event with rainfall intensity of 133.5 mm/hr happened in June 2008, substantial down-slope movement was recorded at all depths. The displacement in response to this particular storm event was 30 – 40 mm by IPI<sub>ce</sub> and 15 – 25 mm by IPI<sub>th</sub>. When rainfall with intensity larger than 30 mm/hr happened after the storm, almost immediate down-slope displacements (~5 mm) were recorded in the top 3 m of the slope by both IPIs. As the rain ceased, the displacement at each depth reduced (i.e., rebounded towards up-slope direction), at a much slower rate, to its initial level before the rainfall. As compared to the responses of PWP (Fig. 6(a)), such deformation pattern may be attributed to the build-up and reduction of positive PWP.

Figure 6(d) compares the variations of total horizontal pressure,  $\sigma_D$  and  $\sigma_C$ , at 2 m depth with time. It

should be noted that the measurements made by both EPCs represent the change of total horizontal stress with reference to the initial zero stress after their installation. Measured response of the positive PWP at 1.5 m is also shown for comparison. It can be observed that during the wet period from May to July 2008, the variation of  $\sigma_C$  appears to have a fairly good agreement with that of positive PWP. This suggests that the measured changes of  $\sigma_C$  were attributed to the changes of positive PWP upon rainfalls. On the other hand, the measured  $\sigma_D$  exhibited similar trend to the measured  $\sigma_C$ , but the magnitude of  $\sigma_D$  was always higher. After the storm event on June, the difference between  $\sigma_D$  and  $\sigma_C$  (15 kPa) increased substantially, and this difference appeared to remain similar for the rest of the wet period. Since the two EPCs were installed next to each other at the same depth, they likely recorded similar positive PWP. This implies that the measured higher  $\sigma_D$  is attributed to not only the increase in positive PWP, but also some mobilisation of soil stress.

#### *Effects of PWP on slope deformation characteristics*

Fig. 7 correlates PWP at 0.5, 1.5, and 2.5 m depths with down-slope displacements at 0, 1, and 3 m depths, respectively. During the rainfalls on 6 June, a noticeable increase in horizontal displacement of the slope was recorded when critical PWP at 0.5, 1.5, and 2.5 m depths reached 2, 11, and 15 kPa, respectively. As the slope displaced towards the down-slope direction during the storm event on 7 June, the peak positive PWPs at all three depths, however, remained almost unchanged. This is not expected because results from triaxial tests (Meilani et al. 2005) conducted under constant deviatoric stress, decreasing suction path (commonly referred to as field stress path upon rainfall infiltration) showed that soil deformed simultaneously with PWP changes in both the saturated and the unsaturated states. The field observation seems to suggest that the increase in the positive PWP in shallow depths (top 3 m) could not be the major reason leading to the large observed down-slope displacements.

Daily horizontal displacement profiles measured from 5 – 9 June 2008 are compared in Fig. 8. During the small rainfall occurred on 6 June, a cantilever mode of displacement profile is observed for both IPIs. This displacement mode means that the peak change of displacement occurred at the slope surface, and the change decreased with an increase in depth. After the storm event (i.e., 8 June), significant large down-slope displacements were recorded at all depths in IPI<sub>ce</sub> (Fig. 8(a)). This indicates that the influence depth of slope displacement due to the storm was deeper than 5 m. In order to identify the influence depth, a manual inclinometer survey up to 15 m depth was conducted and two extra accelerometers were installed at 7 and 10 m depths in January 2009. The manual measurement shows that the slope at this particular location exhibited a

deep-seated mode of displacement. A remarkably large displacement of 20 mm was recorded within a stratum between 5.5 and 6 m depths, which is equivalent to an average shear strain of 8%. Considering the fact that the slope displacement profiles before (7 June) and after (8 June) the storm were almost parallel, the landslide body was likely to have undergone a translational type of down-slope displacement along some rupture surfaces developed or/and re-activated at 5.5 – 6 m depth. This is consistent with the building up of positive PWP at these depths when there was significant rise of GWL to an elevation close to the slope surface during the storm (Fig. 2). Such translational movement of the top 5 m of the sliding mass may explain why the peak positive PWPs did not correspond to the peak slope displacements when focusing only the responses in the top 3 m of the slope (Fig. 7).

#### *Stress mobilisation*

Fig. 9 shows the process of stress mobilisation at 2 m depth during slope displacement from 5 – 9 June 2008. The down-slope displacement expressed in x-axis is taken to be the average of the measurements made at 1 and 3 m depths. Since positive PWP and saturated VWC was recorded at 2.5 m depth during the storm event (see Figs 6(a) and (b)), effective stress,  $\sigma_D'$ , can therefore be determined by the difference between  $\sigma_D$  and positive PWP by setting  $\chi$  in Eq. 1 to be 1, as a first approximation. Initially, at zero slope displacement, the  $\sigma_D$  and  $\sigma_D'$  were both 5 kPa and they were attributed to the stress mobilisation during a previous rainfall (intensity up to 60 mm/hr) that happened on April 2008 (see Fig. 6(d)). As shown in Fig. 9(a), the displacement of 5 mm during the small rainfall events on 6 June caused rather stiff response of  $\sigma_D$ , but  $\sigma_D'$  was not mobilised (Fig. 9(b)). This is because the increase in  $\sigma_D$  was mostly attributed to the increase in positive PWP.

As the slope displaced further from 5 to 35 mm during the storm, a 350% increase in  $\sigma_D'$  (from 4 to 14 kPa) was recorded. By the Rankine theory (modified to consider the sloping ground condition) and using the effective strength parameters ( $c'$  of 7.4 kPa and  $\phi'$  of 33°), it may be estimated that the peak  $\sigma_D'$  mobilised almost 40% of the effective passive stress (38 kPa) of CDT. The mobilisation of  $\sigma_D'$  due to the horizontal slope displacement might be analogous to a horizontal subgrade reaction problem. By determining the gradient of the linear portion of the  $\sigma_D'$  curve, it may be deduced that the coefficient of horizontal subgrade reaction,  $\eta_h$ , of the silty clay is 360 kN/m<sup>3</sup>. This value is close to the lower range of  $\eta_h$  (350 – 700 kN/m<sup>3</sup>) of clayey soil (Tomlinson and Woodward 2007). Interestingly, when considering the range of displacement (5 – 35 mm) that mobilised  $\sigma_D'$  in Fig. 7, this range corresponds to the constant responses of positive PWP. The inter-relationship between PWP,  $\sigma_D'$ , and displacement suggests that during the translational sliding of the landslide mass (Fig. 8(a)), the sliding

mass in the top 5 m of the slope may have exhibited substantial deformation that caused the observed mobilisation of  $\sigma_D'$  at 2 m depth.

As the storm ceased on 8 June, the mobilised  $\sigma_D'$  remained almost unchanged at the peak value of 14 kPa, as the landslide body rebounded slightly ( $< 5$  mm) towards the up-slope direction (see Fig. 9(b)). This is because the decrease in  $\sigma_D$  during this period was almost identical to the reduction of positive PWP.

## **Interpretation of slope behaviour during drying period**

### *Observed slope responses during the dry season*

During the dry season from October 2008, negligibly small rainfall was recorded (Fig. 6(a)). At all depths, a substantial decrease of PWP was observed due to plant evapotranspiration and downward water drainage. This caused a corresponding reduction of VWC (Fig. 6(b)). However, due to the cavitation of water in each tensiometer, any suctions higher than 90 kPa could not be recorded. A column drainage experiment conducted by Sakaki et al. (2011) showed that the (gauge)  $u_a$  directly measured in both fine and coarse sand was always within  $\pm 1$  kPa during draining process. Given that the accuracy limit of the JFT used in this field study is also  $\pm 1$  kPa, any change of  $u_a$  during the drying process is considered to be negligible. It is, therefore, reasonable to assume  $u_a$  to be atmospheric (i.e., gauge  $u_a = 0$ ), so that negative PWP measured during the dry season may be taken to be equal to matric suction for interpreting the slope response.

Because of suction recovery, it is evident in Fig. 6(c) that both  $IPI_{ce}$  and  $IPI_{th}$  installed at two different locations of the landslide body showed simultaneous decrease in displacement (i.e., up-slope rebound) by about 10 mm in the top 1 m in five months. This means that up to 25% – 50% of down-slope movements resulted during the storm event on 7 June 2008 was recovered partly. On the contrary, the soil displacements recorded below 3 m depth remained almost constant at both locations. This kind of up-slope displacement was similarly observed from field data reported by Ng et al. (2003) on a clay slope (i.e., 2 mm in two weeks) and by Cheuk et al. (2009) on a decomposed soil slope (i.e., 8 mm in seven months), as well as centrifuge test results reported by Take and Bolton (2011) on a kaolin slope (i.e., 7 mm in seven months; in prototype). Since only two IPIs were installed in the slope, the study is unable to conclude whether the observed up-slope displacement of the slope was localized or as a block for the entire slope. Nevertheless, the centrifuge model tests conducted by Take and Bolton (2011) revealed that the up-slope displacement of their kaolin slope was not localized but happened along the entire slope. As a result of the up-slope rebound in this study, the  $\sigma_D$  reduced gradually from 20 to 0 kPa, while the  $\sigma_C$  remained apparently constant at 0 kPa (Fig. 6(d)).

## *Effects of pore-water pressure on slope displacement*

Fig. 10 relates the horizontal displacements recorded at 0, 1, and 3 m (from IPI<sub>ce</sub>) with suctions measured at 0.5, 1.5, and 2.5 m depths, respectively. As suction increased from 10 to 90 kPa during the drying period, up-slope displacement happened at all of the depths but at a decreasing rate. When compared to the laboratory measurements of the shrinkage of colluvium and CDT, it is interesting to observe that the void ratio of the specimen loaded at net stresses of 0 and 40 kPa reduced at very similar rates as the field measurements made at 0.5 and 2.5 m depths, respectively. Note that the experimental data shown in this figure are the same set of those presented in Fig. 5(b), but expressed on a linear scale for suction on the x-axis. For the same given increase in suction from 10 to 90 kPa, the increase in up-slope displacement (6.3% at the ground surface and 4.3% at 3 m depth) in the field is found to be close to the decrease in void ratio (6.1% at 0 kPa and 4.1% at 40 kPa of net stress) in the laboratory. The close variation suggests that the suction-induced soil shrinkage was probably the most likely reason for up-slope rebound in the dry season. It is worth noting that the up-slope rebound (i.e., ~ 10 mm in five months) occurred at a much slower rate than the down-slope displacement happened during the storm (i.e., > 25 mm in one day; Fig. 6(c)). Such a large contrast in the rate of slope movement between the wet and dry seasons is the primary reason causing the net down-slope movement after one year of monitoring.

## *Slope deformation characteristics and stress mobilisation*

Figs 11(a) and (b) shows the monthly displacement profiles monitored by IPI<sub>ce</sub> and IPI<sub>th</sub>, respectively, during the drying period between October 2008 and March 2009. It can be seen that at both instrument locations, the displacements in the top 5 m depth reduced, whereas the soil below 7 m was largely stationary. The observed decreases in displacement indicate that the soil displaced towards the up-slope direction during the drying period. This is referred to as up-slope rebound. The large displacement at 5.5 – 6 m previously recorded at IPI<sub>ce</sub> is found to be almost irrecoverable. This supports the preceding discussion that rupture surfaces were likely to have developed or/and re-activated during the heavy rainstorm happened on June 2008. It can be identified that at both locations, the reduction of displacement was smaller in deeper depths. This shape of deformation may be the consequence of the decrease of shrinkability of soil with an increase in depth. As shown in Fig. 5(b), soil subjected to a higher vertical load (equivalent to overburden pressure in the field) has a lower reduction in the void ratio due to a higher soil stiffness. As the vertical load increased from 0 to 80 kPa (equivalent to an increase in depth from 0 to 4 m), the decrease in void ratio reduced from 7.2% to 3.5%.

As the slope rebounded from 34 to 29 mm, it can be seen in Fig. 9(a) that  $\sigma_D$  built up during the previous storm reduced substantially from 20 to 0 kPa (i.e., restoring to the initial value of  $\sigma_D$  after the installation of the EPC). Since the EPC reached their minimum measurable values, no further stress relief can be recorded beyond December 2008 even though there was continuous up-slope movement from the 29 mm on January 2009 to 25 mm on March 2009 (see Fig. 6(c)). As suction developed and VWC dropped below the saturated value during the drying period,  $\sigma_D'$  can be evaluated by Eq. 1 using the value of  $\chi$  in relation to the suction,  $s$ . As the EPC was installed at 2 m depth, the suction used to calculate  $\sigma_D'$  in Eq. 1 is taken to be the average suction recorded by the JFTs installed at 1.5 and 2.5 m depths. On the other hand, the  $s_e$  (i.e., AEV) is taken to be 2 kPa. It can be seen in Fig. 9(b) that the  $\sigma_D'$  decreased as the slope rebounded. Although the increase in suction during the dry season contributed to some increase in  $\sigma_D'$ , the overall reduction of  $\sigma_D'$  was because of much more significant reduction of  $\sigma_D$  during the up-slope rebound. Moreover, a stiffer response of  $\sigma_D'$  during the dry season is observed, as compared to that observed during the wet season. This is consistent with the general soil behaviour that soil stiffness following an unloading path (during the dry season in this case) within a yield surface is stiffer than that following a loading path (during the wet season) at the yield surface (Ng and Xu 2012). This indicates that the mobilisation of  $\sigma_D'$  during the wet season was likely a plastic process that caused the irrecoverable displacement after a cycle of wet/dry season (Fig. 11(a)).

## Summary and conclusions

In this study, a full-scale field monitoring was conducted to investigate seasonal stress mobilisation and deformation characteristics of a saprolitic soil slope. The research slope was heavily instrumented to monitor the responses of not only PWP and groundwater level, but also the horizontal stress and the horizontal displacement. To assist in the interpretation of field data, a series of laboratory tests was conducted to quantify the effects of net stress and suction on the water retention ability and the volume change behaviour of soil taken from the slope.

During an extreme storm event (return period equivalent to 245 years), it is identified that the slope exhibited a deep-seated mode of displacement. A remarkably large displacement of 20 mm was recorded within a stratum between 5.5 and 6 m depths as significant positive PWP was built up by the rise of groundwater table. It is evident that the top 5 m of the slope exhibited translational down-slope movement, whereas the slope at depths below 7 m remained largely stationary. During the down-slope movement, an effective horizontal stress (determined by the difference of total horizontal stress measured by earth pressure cell and positive PWP

recorded by tensiometer) was found to be mobilised by 350% (i.e., from 4 to 14 kPa), which reached a peak value equivalent to 40% of an effective passive stress. This indicates that during the translational sliding of the landslide mass, the sliding mass exhibited substantial deformation that caused the significant stress mobilisation.

During the subsequent dry season, up-slope rebound movement is observed, but not more than 25% (i.e., 10 mm) of the down-slope displacement resulting from the extreme storm was recovered. For a given increase in suction, it is revealed that the increase in up-slope displacement (4.3% – 6.3%) in the field was close to the decrease in void ratio (4.1% – 6.1%) of soil tested at similar overburden stress levels in the laboratory. This evidently suggests that the up-slope rebound was attributed to soil shrinkage due to suction recovery. Since the soil shrinkability reduced with an increase in overburden stress, smaller up-slope displacement was observed at deeper depths. This led to a cantilever shape of up-slope displacement profile. Due to the up-slope rebound, all of effective horizontal stress built up during the previous storm event was recovered.

## Acknowledgements

The first author would like to acknowledge the research grant provided by the Career Integration Grant through the EU Marie Curie Fellowship under the project “BioEPIC slope”, as well as the research travel fund supported by the Northern Research Partnership (NRP). The research grant HKUST6/CRF/12R provided by the Research Grants Council of the Government of the HKSAR and research grant (2012CB719805) from the National Basic Research Program (973 Program) provided by the Ministry of Science and Technology of the People's Republic of China are also acknowledged. The authors would like to acknowledge the Geotechnical Engineering Office (GEO), Civil Engineering and Development Department (CEDD), the Government of the HKSAR for funding the field monitoring work presented in this paper. The Head of GEO and the Director of CEDD are acknowledged for the permission to use of the base photograph in Fig. 1.

## References

- AECOM (2012) Detailed study of the 7 June 2008 landslides on the hillside above the North Lantau Highway and Cheung Tung Road, North Lantau. GEO Report No. 272, Geotechnical Engineering Office, Civil Engineering Department, The Government of the Hong Kong Special Administrative Region
- Brackley IJA, Sanders PJ (1992) In-situ measurement of total natural horizontal stresses in an expansive clay. *Geotechnique* 42(2):443-451
- BSI (2004) BS EN 1997-1:2004: Eurocode 7: Geotechnical design. General rules. BSI, London, UK.

- 1 Cheuk J, Ng A, Endicott J, Ho K (2009) Progressive slope movement due to seasonal wetting and drying. Proc.  
2 Seminar on “The State-of-the-art Technology and Experience on Geotechnical Engineering in Malaysia and  
3 Hong Kong”. The HKIE Geotechnical Division, 25 February 2009, Hong Kong, pp 105-114
- 4 Coleman JD (1962) Correspondence: stress/strain relations for partly saturated soils. *Geotechnique* 12(4):348–  
5 350
- 6 Hilf JW (1956) An investigation of pore-water pressure in compacted cohesive soils. PhD Thesis. Technical  
7 Memorandum No. 654, United State Department of the Interior Bureau of Reclamation, Design and  
8 Construction Division, Denver, Colorado, USA
- 9 IPCC (2007) Summary for Policymakers. In: *Climate Change 2007: The Physical Science Basis. Contribution*  
10 *of Working Group I to the Fourth Assessment Report of the Intergovernmental Panel on Climate Change.*  
11 Cambridge University Press, Cambridge, United Kingdom and New York, NY, USA.
- 12 Khalili N, Khabbaz MH (1998) A unique relationship for  $\chi$  for the determination of the shear strength of  
13 unsaturated soils. *Geotechnique* 48(2):1–7
- 14 Kim YK, Lee SR (2010) Field infiltration characteristics of natural rainfall in compacted roadside slopes.” *J*  
15 *Geotech Geoenviron Eng* 136(1):248-252
- 16 Leung AK, Ng CWW (2013a) Seasonal movement and groundwater flow mechanism in an unsaturated saprolitic  
17 hillslope. *Landslides* 10(4):455-467
- 18 Leung AK, Ng CWW (2013b) Analysis of groundwater flow and plant evapotranspiration in a vegetated soil  
19 slope. *Can Geotech J* 50(12):1204-1218
- 20 Leung AK, Sun HW, Millis SW, Pappin JW, Ng CWW, Wong HN (2011) Field monitoring of an unsaturated  
21 saprolitic hillslope. *Can Geotech J* 48(3):339-353
- 22 Lim TT, Rahardjo H, Chang MF, Fredlund DG (1996) Effect of rainfall on matric suction in a residual soil slope.  
23 *Can Geotech J* 33(2):618-628
- 24 Meilani I, Rahardjo H, Leong EC (2005) Pore-water pressure and water volume change of an unsaturated soil  
25 under infiltration conditions. *Can Geotech J* 42(6):1509-1531
- 26 Ng CWW, Pang YW (2000) Experimental investigations of the soil-water characteristics of a volcanic soil. *Can*  
27 *Geotech J* 37(6):1252-1264.
- 28 Ng CWW, Xu J (2012) Effects of current suction ratio and recent suction history on small strain behaviour of an  
29 unsaturated soil. *Can Geotech J* 49(2):226-243
- 30 Ng CWW, Yung SY (2008) Determination of the anisotropic shear stiffness of an unsaturated decomposed soil.
-



1 Géotechnique 58(1):23-35

2 Ng CWW, Zhan LT, Bao CG, Fredlund DG, Gong BW (2003) Performance of an unsaturated expansive soil  
3 slope subjected to artificial rainfall infiltration. *Geotechnique* 53(2):143-157

4 Ng CWW, Wong HN, Tse YM, Pappin JW, Sun HW, Millis SW, Leung AK (2011) A field study of  
5 stress-dependent soil-water characteristic curves and permeability of a saprolitic slope in Hong Kong.  
6 *Geotechnique* 61(6):511-521

7 Sakaki T, Limsuwat A, Illangasekare TH (2011) An improved air pressure measuring method and demonstrated  
8 application to drainage in heterogeneous soils. *Vadose Zone J* 10(2):706-715

9 Sassa K, Canuti P (2008) *Landslides – Disaster risk reduction*, Springer, New York.

10 Smethurst JA, Clarke D, Powrie W (2006) Seasonal changes of pore water pressure in a grass-covered cut slope  
11 in London clay. *Geotechnique* 56(8):523-537

12 SMO (1995) *Explanatory Notes On Geodetic Datums in Hong Kong*. Survey and Mapping Office (SMO),  
13 Lands Department, the Government of the HKSAR, Hong Kong.

14 Take WA, Bolton MD (2011) Seasonal ratcheting and softening in clay slopes, leading to first-time failure.  
15 *Geotechnique* 61(9):757-769

16 Tomlinson M, Woodward J (1994) *Pile design and construction practice*. 5<sup>th</sup> Ed., CRC Press, Taylor and Francis  
17 Group, Florida

18 van Genuchten, MTh (1980) A closed-form equation for predicting the hydraulic conductivity of unsaturated  
19 soils. *Soil Sci Soc Am J* 44(5):892–898.

1 **LIST OF CAPTIONS**

2 **LIST OF TABLES**

---

Table 1 A summary of soil properties

---

Table 2 A summary of coefficients for fitting the laboratory measured SWRCs using the equation proposed by van Genuchten (1980)

---

3

4 **LIST OF FIGURES**

---

**Fig. 1** Overview of the research slope (Note: Base photograph sourced from the website of Hong Kong Slope Safety (HKSS) managed by the Geotechnical Engineering Office, Civil Engineering and Development Department, HKSAR)

---

**Fig. 2** Ground profile and arrangement of instruments

---

**Fig. 3** Particle-size distributions of colluvium and CDT

---

**Fig. 4** Mohr-Coulomb failure envelopes of (a) colluvium and (b) CDT determined from triaxial CU tests

---

**Fig. 5** (a) Soil water retention curves (SWRCs) and (b) suction-induced shrinkage behaviour of colluvium at zero net stress and CDT at net stresses of 40 and 80 kPa

---

**Fig. 6** Measured variations of (a) pore-water pressure, (b) volumetric water content, (c) total horizontal displacement, and (d) total horizontal stress with rainfall intensity during the monitoring period from April 2008 to March 2009

---

**Fig. 7** Relationships between pore-water pressure and total horizontal displacement during the storm event from 5 to 9 June 2008

---

**Fig. 8** Measured total horizontal displacement profiles during the storm event (a) at the central portion ( $IPI_{ce}$ ) and (b) near the thrust features ( $IPI_{th}$ ) of the landslide body

---

**Fig. 9** Observed stress mobilisation upon total horizontal displacements during the storm event from 5 – 9 June 2008 and during drying period from October to December 2008, in terms of (a) total stress, and (b) effective stress

---

**Fig. 10** Relationships between pore-water pressure and total horizontal displacement during the drying period from October to December 2008

---

**Fig. 11** Measured total horizontal displacement profiles during the drying period (a) at the central portion ( $IPI_{ce}$ ) and (b) near the thrust features ( $IPI_{th}$ ) of the landslide body

---

5

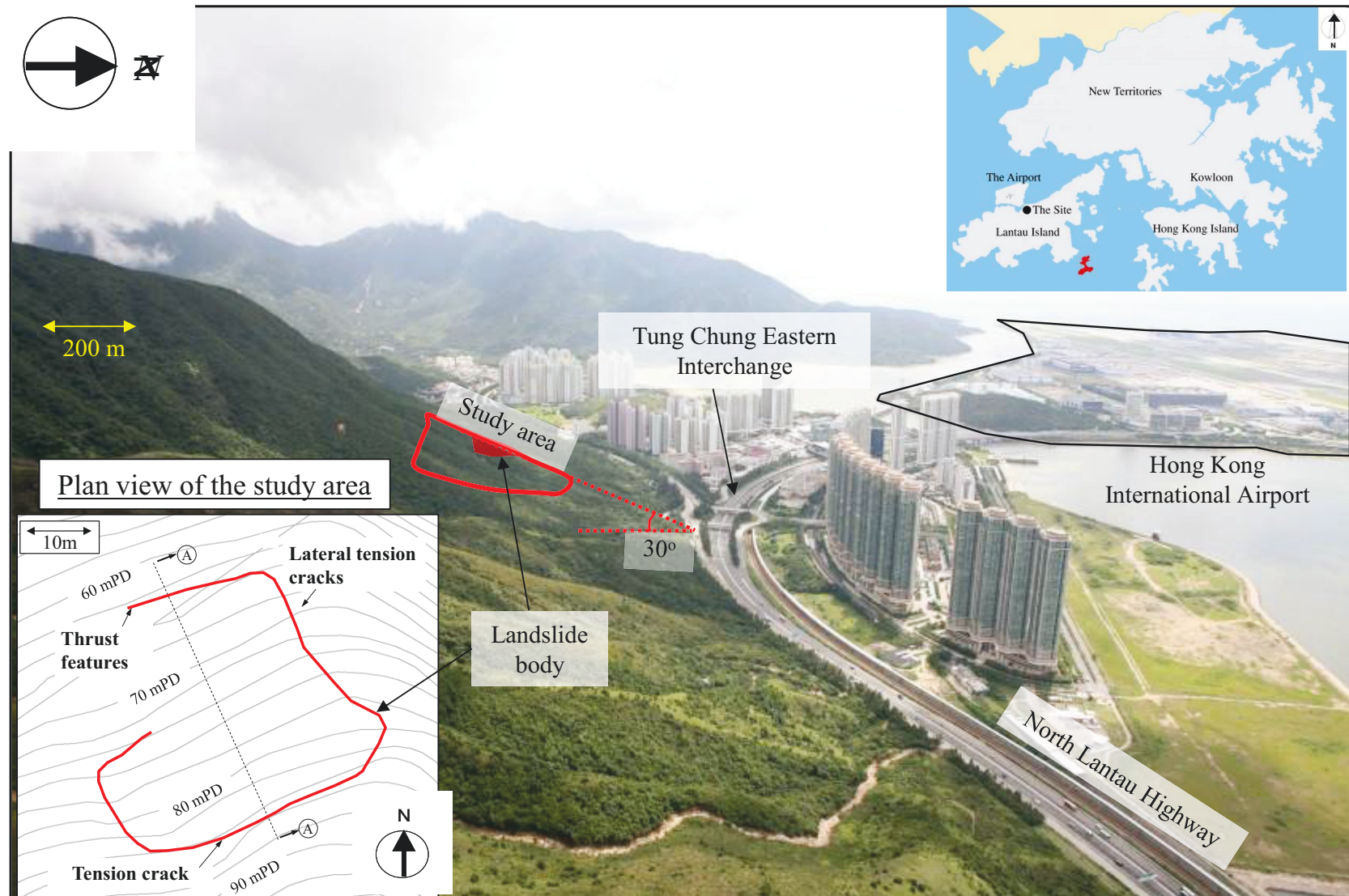
6

1 Table 1. A summary of soil properties

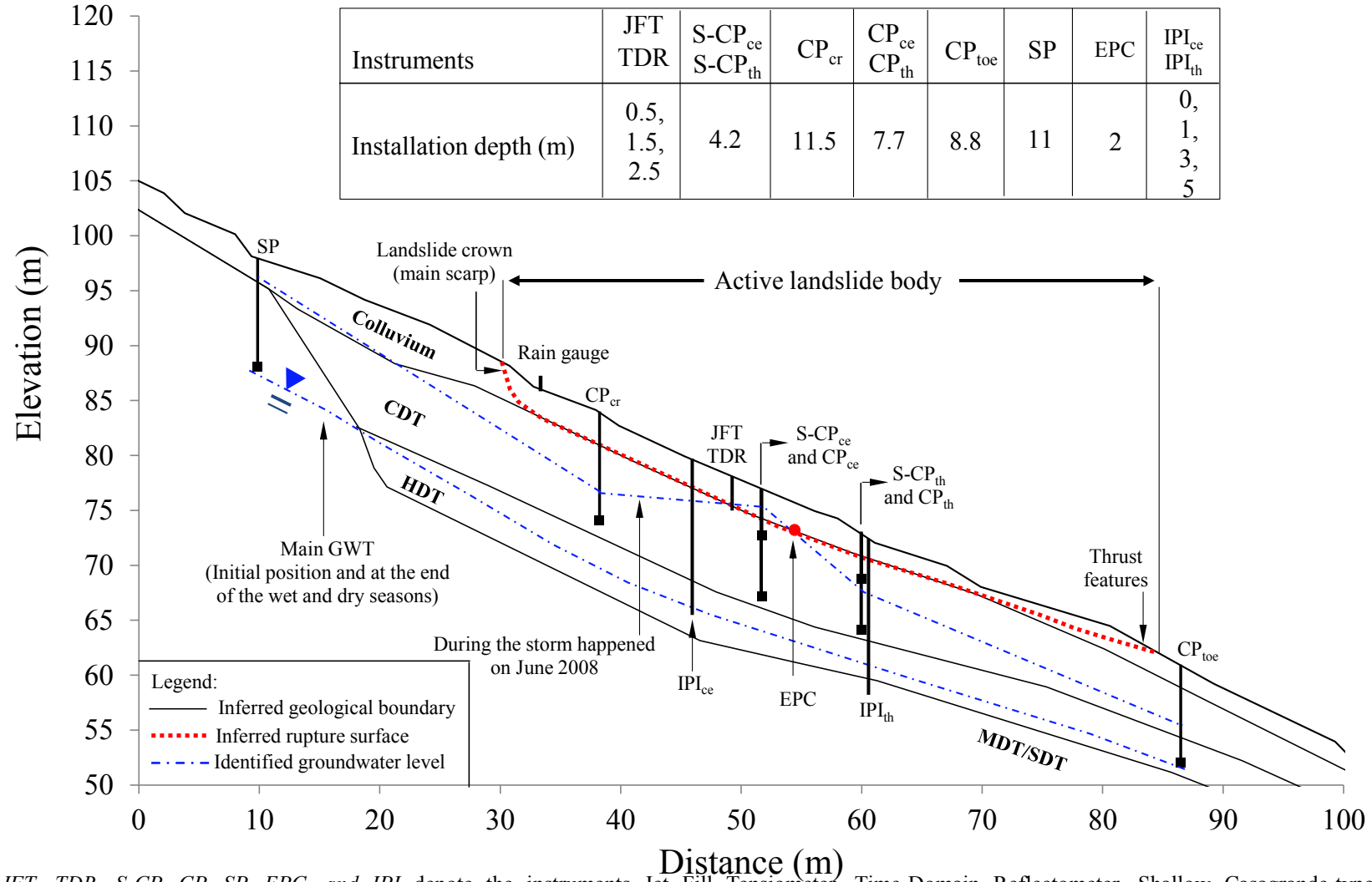
Measured index properties	Colluvium	CDT
<i>Compaction properties</i>		
Maximum dry density (g/m <sup>3</sup> )	1.58	1.78
Optimum water content (%)	15.2	17.3
<i>Particle-size distributions</i>		
Gravel content ( $\geq 2$ mm, %)	18	2.5
Sand content (63 $\mu$ m – 2 mm, %)	25.5	35
Silt content (2 $\mu$ m – 63 $\mu$ m, %)	39.5	42.5
Clay content ( $\leq 2\mu$ m, %)	17	20
<i>Atterberg limit</i>		
Liquid limit (%)	41	34
Plastic limit (%)	17	20
Plasticity index (%)	24	14
<i>Strength parameters</i>		
Effective cohesion, $c'$ (kPa)	0.3	7.4
Effective frictional angle, $\phi'$ (°)	35.2	33
Specific gravity	2.73	2.68
	CL	CL
Unified Soil Classification System	(sandy lean clay with gravel)	(Sandy lean clay)

1 Table 2. A summary of coefficients for fitting the laboratory measured SWRCs using the  
2 equation proposed by van Genuchten (1980)

Soil type	Net stress (kPa)	Drying/Wetting	Fitting coefficients				
			$\alpha$	$n$	$m$	$\theta_s$	$\theta_r$
			(kPa <sup>-1</sup> )			(m <sup>3</sup> /m <sup>3</sup> )	(m <sup>3</sup> /m <sup>3</sup> )
Colluvium	0	Drying	0.8	1.2	0.167	0.409	0.049
		Wetting	1.2	1.5	0.333	0.394	0.192
CDT	40	Drying	0.3	1.5	0.333	0.390	0.195
		Wetting	3	1.4	0.286	0.380	0.220
	80	Drying	0.3	1.5	0.333	0.384	0.223
		Wetting	4	1.4	0.286	0.376	0.239



1  
2 **Fig. 1** Overview of the research slope (Note: Base photograph sourced from the website of Hong Kong Slope Safety (HKSS) managed by the  
3 Geotechnical Engineering Office, Civil Engineering and Development Department, HKSAR)



Note: *JFT*, *TDR*, *S-CP*, *CP*, *SP*, *EPC*, and *IPI* denote the instruments Jet Fill Tensiometer, Time-Domain Reflectometer, Shallow Casagrande-type Piezometer, Casagrande-type Piezometer, Standpipe, Earth Pressure Cell, and In Place Inclinator, respectively. The subscript *cr*, *ce*, *th*, and *toe* denote the installation location of instrument near the crest, at the central portion, near the thrust feature, and near the toe of the slope, respectively.

**Fig. 2** Ground profile and arrangement of instruments

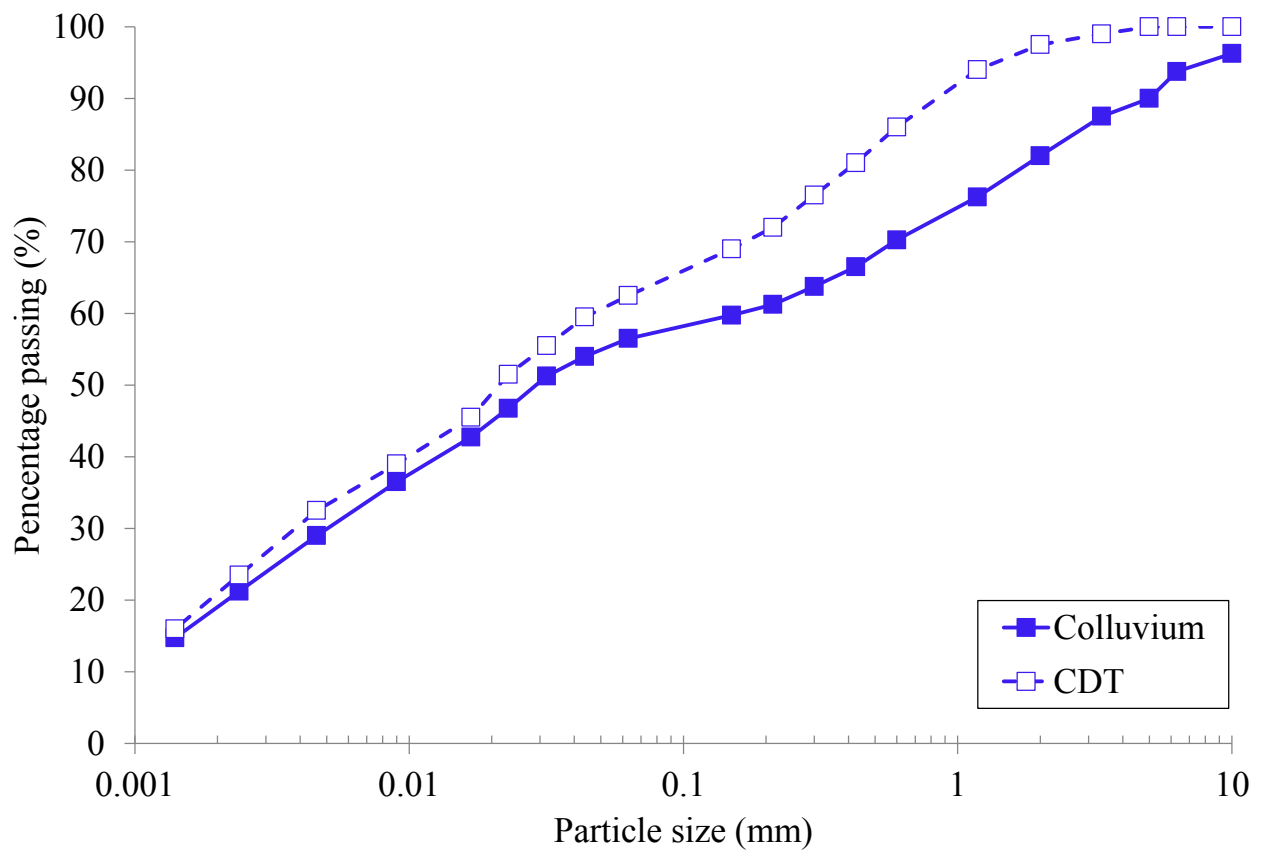


**Fig. 3** Particle-size distributions of colluvium and CDT

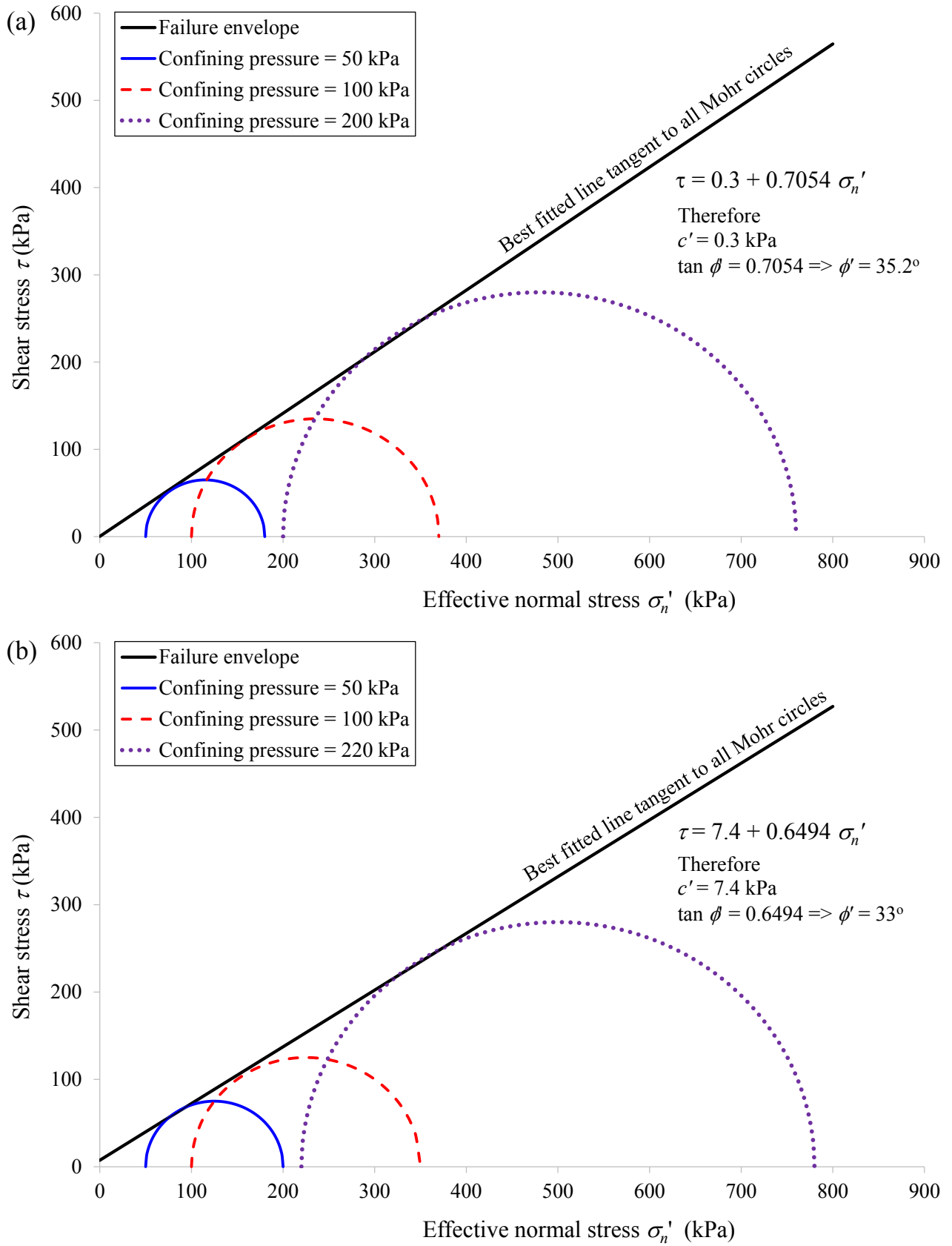


**Fig. 4** Mohr-Coulomb failure envelopes of (a) colluvium and (b) CDT determined from triaxial CU tests



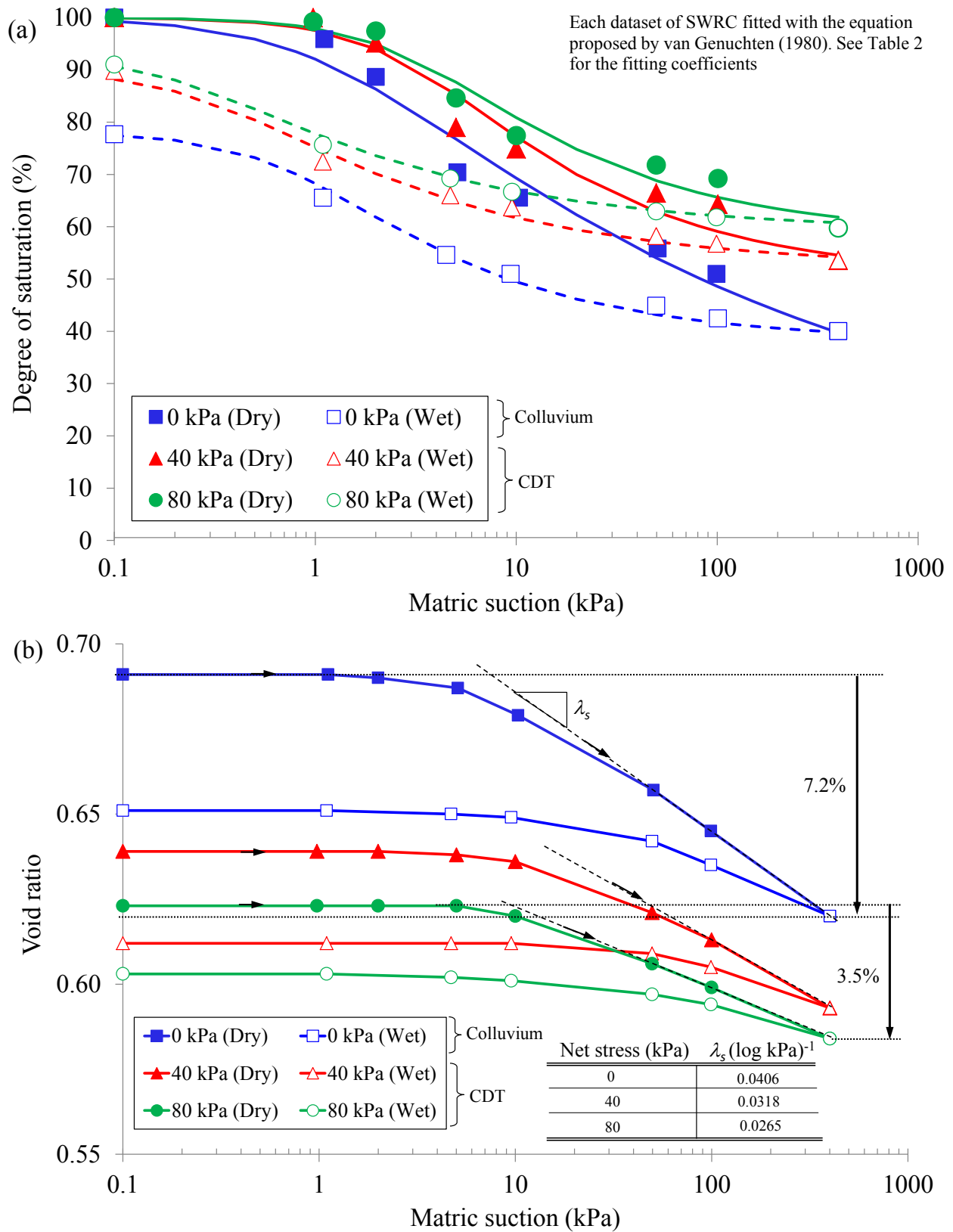


**Fig. 5** (a) Soil water retention curves (SWRCs) and (b) suction-induced shrinkage behaviour of colluvium at zero net stress and CDT at net stresses of 40 and 80 kPa

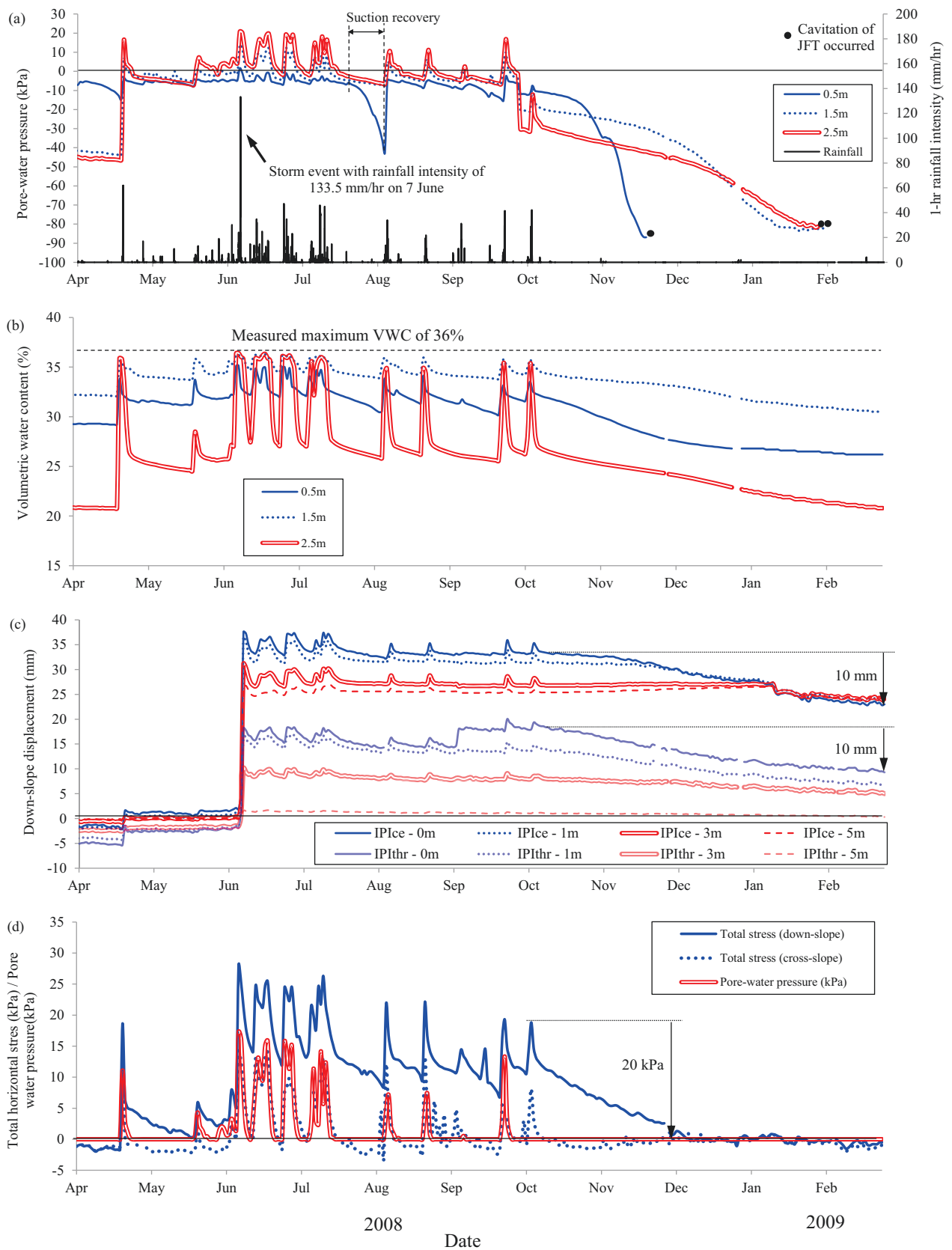


**Fig. 6** Measured variations of (a) pore-water pressure, (b) volumetric water content, (c) total horizontal displacement, and (d) total horizontal stress with rainfall intensity during the monitoring period from April 2008 to March 2009

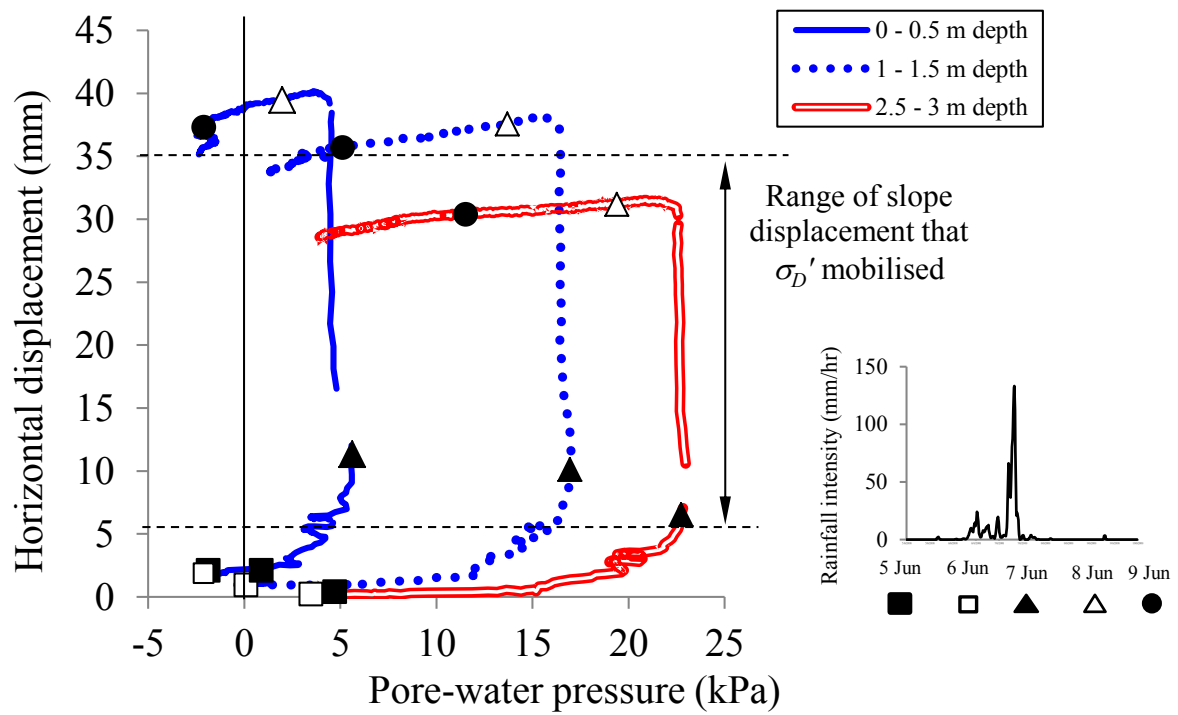


**Fig. 7** Relationships between pore-water pressure and total horizontal displacement during the storm event from 5 to 9 June 2008

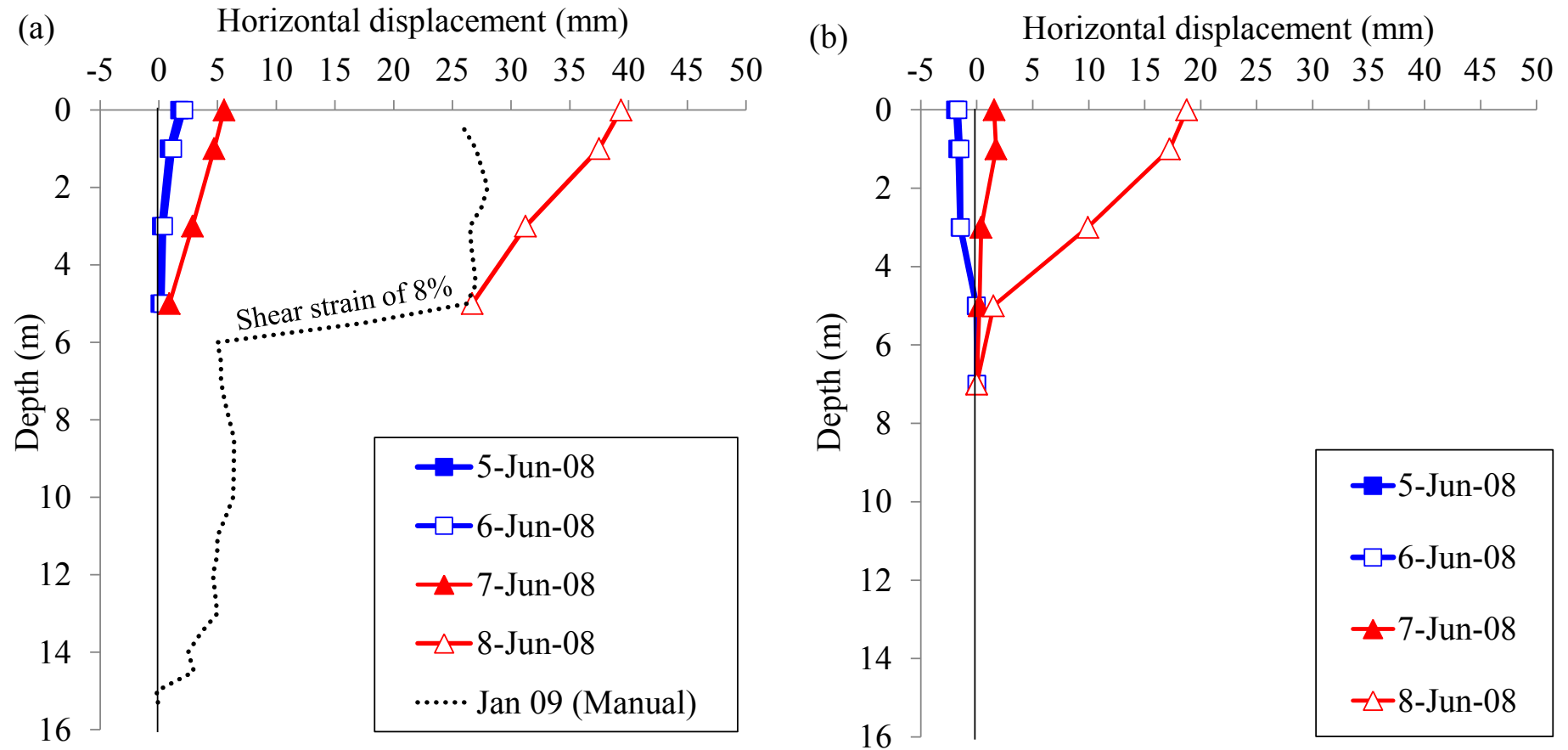


**Fig. 8** Measured total horizontal displacement profiles during the storm event (a) at the central portion (IPI<sub>cc</sub>) and (b) near the thrust features (IPI<sub>th</sub>) of the landslide body

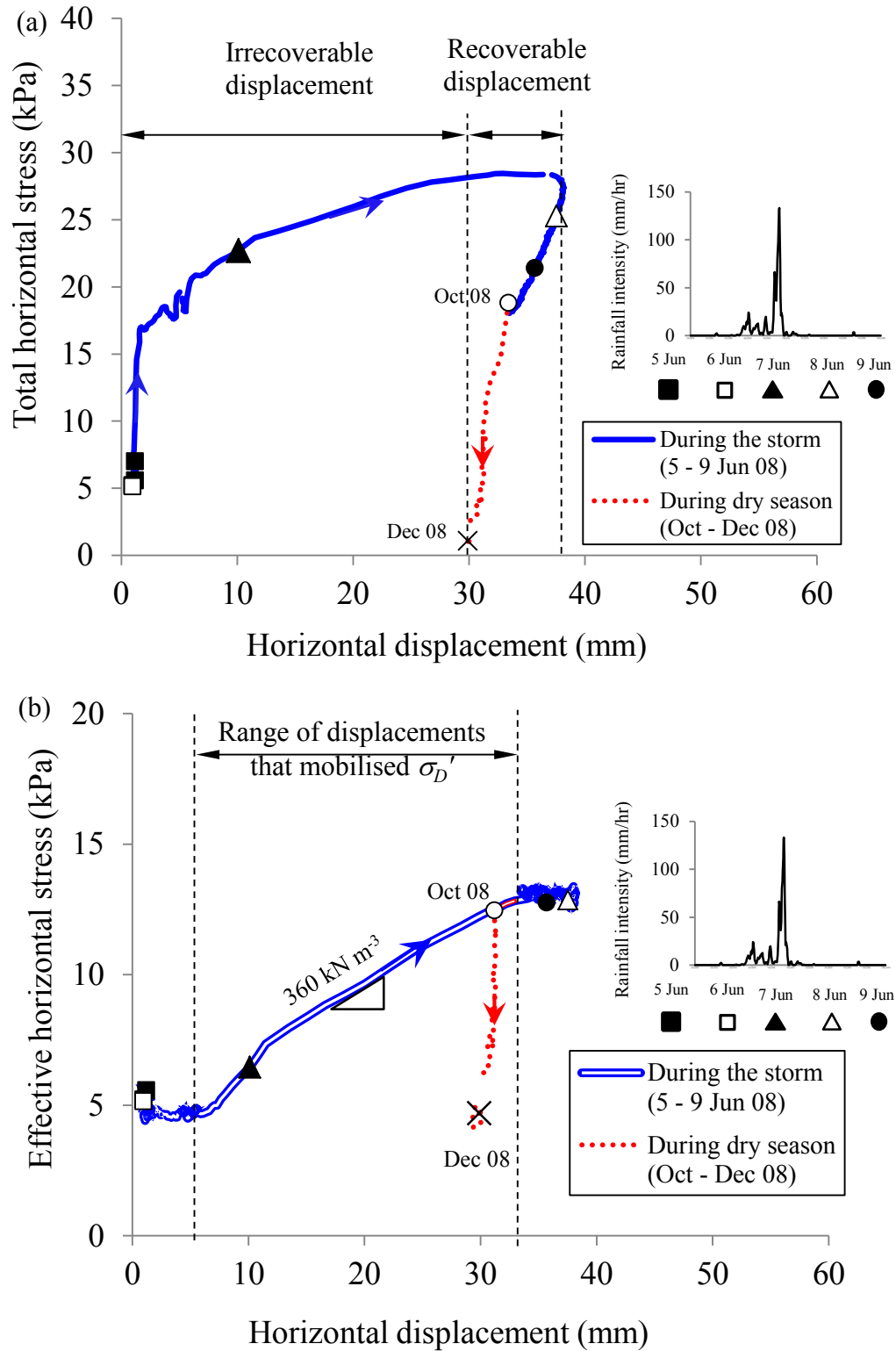


**Fig. 9** Observed stress mobilisation upon total horizontal displacements during the storm event from 5 – 9 June 2008 and during drying period from October to December 2008, in terms of (a) total stress, and (b) effective stress

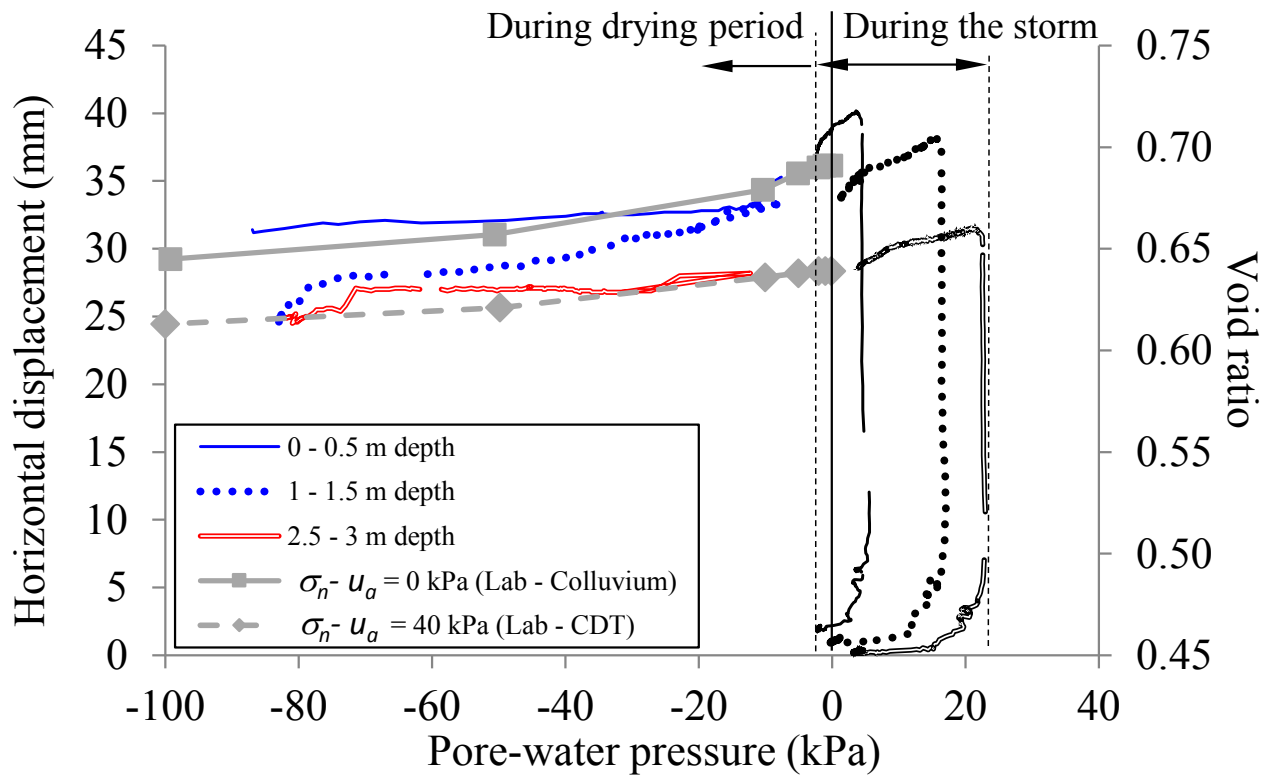


**Fig. 10** Relationships between pore-water pressure and total horizontal displacement during the drying period from October to December 2008

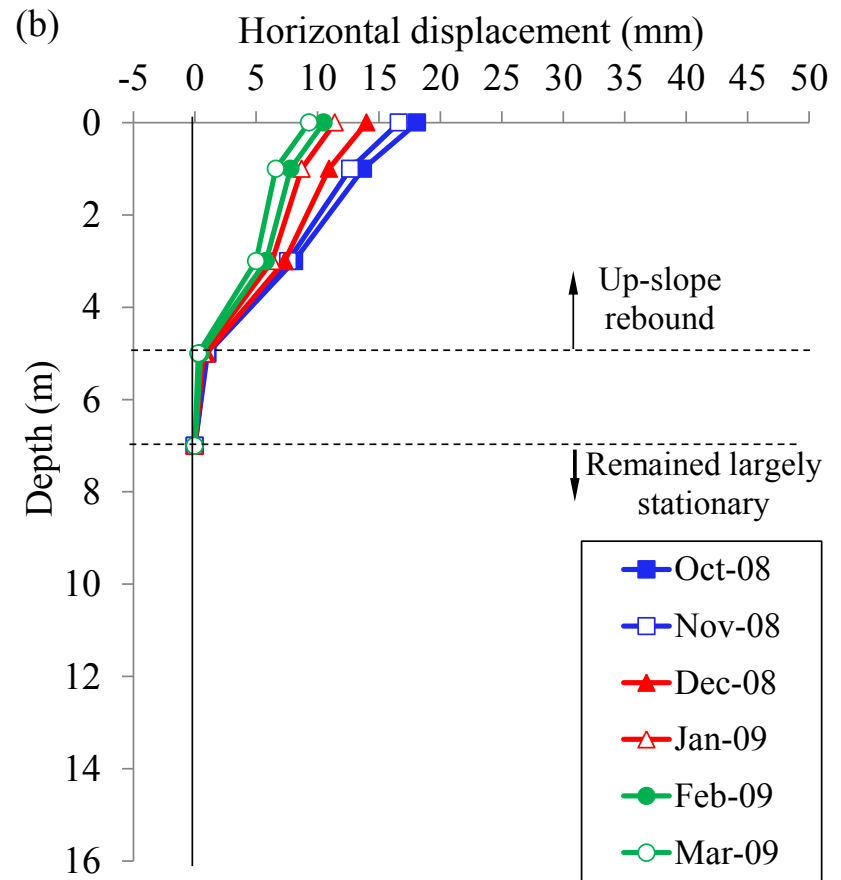
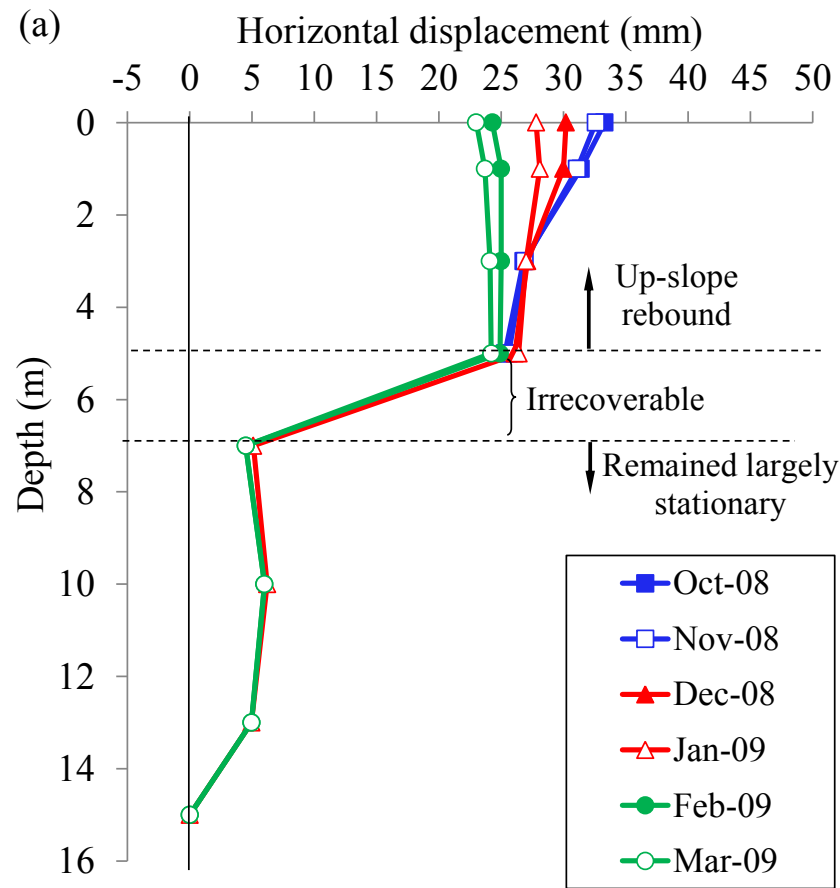


**Fig. 11** Measured total horizontal displacement profiles during the drying period (a) at the central portion ( $IPI_{ce}$ ) and (b) near the thrust features ( $IPI_{th}$ ) of the landslide body